Journal of Chemical Health Risks

www.jchr.org

JCHR (2024) 14(5), 235-247 | ISSN:2251-6727

Green Synthesized Silver Nanoparticles Induce Apoptosis and G2/M Arrest Via Signalling Pathways in MCF-7 Breast Cancer Cell Lines.

Renuka Saravanan and Sivakumar Ramalingam*

Department of Chemistry and Biosciences, SASTRA Deemed to be University, Srinivasa Ramanujan Centre, Kumbakonam 612 001, Tamil Nadu, India.

Corresponding authors' details;
Name: Sivakumar Ramalingam
Affiliation: SASTRA Deemed to be University

(Received: 11 June 2024 Revised: 16 July 2024 Accepted: 10 August 2024)

GRAPHICAL ABSTRACT:

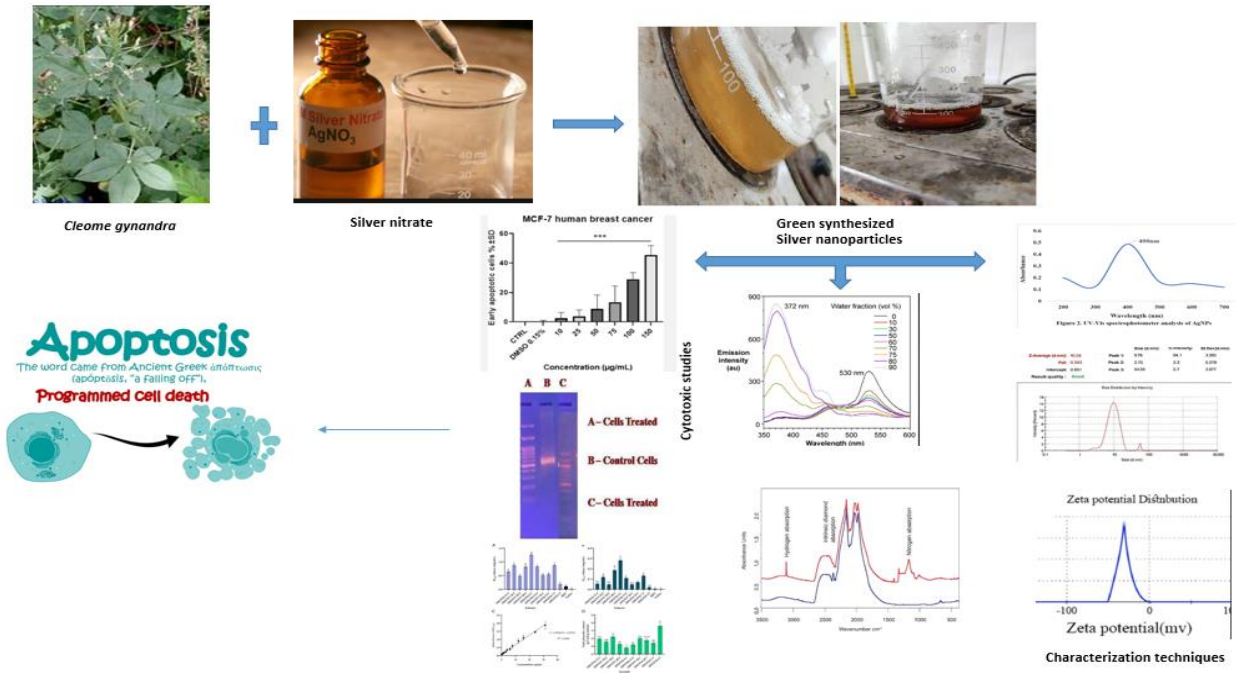

KEYWORDS

Green synthesis, silver nanoparticles, anti-cancerous activity, anti-oxidant activity, MCF-7.

ABSTRACT:

Objective: In the present study, silver nanoparticles (AgNPs) were synthesized from leaf extracts of *Cleome gynandra*, and their anticancer and antioxidant activities were evaluated. **Experimental**: The synthesized silver nanoparticles were characterized by UV-visible spectroscopy (UV-Vis), Scanning Electron Microscope (SEM), Fourier Transform Infrared Spectroscopy (FTIR), Photoluminescence analysis, Zeta Potential, and Particle size analysis. The SEM image showed rod-shaped silver nanoparticles with a diameter range of 520nm. The maximum absorption of silver nanoparticles was recorded at 400nm in UV-visible spectroscopy due to Surface Plasmonic Resonance (SPR). FT-IR spectroscopy

Journal of Chemical Health Risks

www.jchr.org

JCHR (2024) 14(5), 235-247 | ISSN:2251-6727

revealed that silver nanoparticles had different functional groups. Synthesized AgNP was assessed for its antioxidant and cytotoxic effect against MCF-7 cells.

Results: The zeta potential for silver nanoparticles was found to be -18.2 mV which indicated their stability. The photoluminescence results confirmed an excitation peak at 397.07nm and an emission peak at 579.85nm. The synthesized silver nanoparticles were subjected to anticancer and antioxidant activities. Antioxidant results determined by 1,1-diphenyl-2-picrylhydrazyl (DPPH) scavenging assay, hydrogen peroxide assay, and reducing power assay revealed efficient antioxidant potential of the biosynthesized AgNPs. MCF cells treated with the nanoparticle showed a significant decrease in cell viability in a concentration-dependent manner.

Discussion: DNA fragmentation assay showed that the AgNPs induced apoptosis by cleaving nuclear DNA by forming a ladder pattern. Apoptotic activity of the nanoparticles could be due to the accumulation of the AgNPs in the mitochondria and nucleus. They interact with DNA and damage the cells.

Conclusion: Based on the results obtained, it is evident that the aqueous extract of *Cleome gynandra* is an effective reducing agent for the green synthesized AgNPs with antioxidant and anticancer activities, which provides a promising approach for alternative nano-drug development.

Introduction

Nanotechnology is one of the most attractive and widespread technologies in the current century. Nanoparticles (NPs) are technically defined as particles with one dimension less than 100 nm. Nanotechnology is gaining much attention in the fields of nanomedicines, nanoelectronics, biomaterials, energy production, and consumer products. Biosynthesized metal nanoparticles have attracted a lot of attention in recent years because of their interesting properties and potential applications in many different fields. Nanoparticles have unique structural, biological, and optical properties that make them ideal for a variety of applications, including medication administration and biosensors, decreasing the rate of irregular cell proliferation, delaying the spread of infectious agents, and regulating faulty molecular pathways in the body.

Green nanoparticle synthesis is defined as preferring a biological method that includes the use of plants and microorganisms over the use of chemicals. Green synthesis is a fast approach for producing very stable nanoparticles while controlling nanoparticle size and toxicity. When compared to chemical synthesis, green synthesis can limit the creation of poisonous and harmful by-products that can harm the living system, allowing for the synthesis of eco-friendly goods [1]. Nanoparticles of metals like zinc, selenium, cobalt, silver, nickel, and even lead have been the subject of extensive research. Among these, silver has the unique power to increase or decrease biological system regulation and also serves as a tool for detecting and treating bodily problems [2]. AgNPs have gained significant interest in the biomedical field due to their outstanding characteristics as a potential therapeutic approach in the treatment of different types of diseases, such as bacterial and fungal infections, inflammation, and cancers. The green synthesis of AgNPs from natural sources has been demonstrated as significant in reducing the progression of human hepatic cancer cells [3].

Cancer is one of the significant public health problems globally and is the second leading cause of death. It is a generic term for a set of diseases characterized by uncontrolled, random cell division and invasiveness. Despite the traditional therapeutic strategies, lack of specificity, cytotoxicity, and multi-drug resistance pose a substantial challenge to cancer treatment. The advent of nanotechnology has revolutionized the area of cancer diagnosis and treatment. NPs are a growing research tool for overcoming these challenges [4]. Nanomaterials can induce apoptosis through the generation of reactive oxygen species and mitochondrial membrane depolarization during intrinsic apoptosis. In recent years, metal nanoparticles containing herbs have been used to treat cancers of the ovaries, prostate, oesophagus, stomach, lungs, and various leukaemia; it is hypothesized

Journal of Chemical Health Risks
www.jchr.org
JCHR (2024) 14(5), 235-247 | ISSN:2251-6727

that combining metal nanoparticles with medicinal plants will significantly improve their anti-cancer capability [5].

Most of the researchers have concentrated on different methods to synthesize silver nanoparticles, such as chemical, physical, and biological, through chemical reduction, biological materials reduction, and electrochemical reduction [6]. However, physical and chemical reduction-mediated methods have more toxicity and cannot be used in any applications properly, and their usage is also limited [7, 8]. Usually, all biologically mediated nanomaterial synthesis is very efficient, and their biomedical application capacity is also very high. Among these, plant-mediated nanomaterial synthesis is an excellent choice because of the ease of scale-up, cost-effectiveness, and, importantly, non-toxic [9]. Due to these advantages, all the researchers are presently focusing on green synthesized nanomaterials with excellent biomedical applications in various fields [10].

Silver nanoparticles (AgNPs) have gained prominence due to their diverse uses in various industries. AgNPs are among the most intriguing particles due to their unique features in industrial applications. Silver nanoparticles are an essential component of nanotechnology [11]. Silver nanoparticles are also effective against an extensive variety of micro-organisms, including bacteria and fungi, and also in resistant strains for antibiotics. Plant-derived silver nanoparticles are employed not only as antibacterial, antifungal, antiviral, anti-inflammatory, and wound healing properties, diagnostics of cancer, and delivery drugs but also in biological imaging [12].

The most advantages in plant-mediated synthesis are phytochemical derivatives, proteins, hormones, amino acids, bioactive compounds, alkaloids, organic compounds, polysaccharide materials, amino acids, and other plant growth-promoting hormones with their nutrients [13,14]. All these materials act as a reducing and capping agent, which helps to make unique properties, larger surface area, and smaller-sized particles. Among the nanoparticles, the silver nanoparticle is an excellent nanoparticle that has admirable properties in the application fields of biomedical, biopharmaceutical, industrial, food packaging, wastewater treatment, and agricultural fields [15, 16, 17]. In addition, the anti-oxidant and anti-cancer abilities of the green synthesized silver nanoparticle have also been extensively reported [13, 14, 16]

The cytotoxicity effect of the silver nanoparticle on MCF-7 breast cancer cells was demonstrated. The generated silver nanoparticle causes membrane blebbing, cleaves the nucleus, condenses chromatin, generates ROS, damages the mitochondrial membrane, and simulates the death process in MCF-7 breast cancer cells.

Considering all these details, the demand for the advancement of novel strategies for seeking precise therapy for cancer has gained momentum in recent years. Recent efforts have been made to address the limitations of existing therapeutic approaches using nanoparticles. Nanoparticle-based drug delivery systems have reflected benefits in cancer treatment and management by demonstrating good pharmacokinetics, precise targeting, reduced side effects, and drug resistance [4]. Altogether, the present study aims to confirm the anticancer activity of green synthesis of silver nanoparticles performed against MCF-7 human breast cancer cells through cytotoxicity and morphological evidence.

MATERIALS AND METHODS

CHEMICALS

All the chemicals and glass wares of the initial experimental setup were purchased from Merck Scientific & Co with the help of local supplier Ponmani @ Co, Tiruchirappalli, Tamil Nadu, India. The cytotoxicity stain of MTT solution, DMEM medium, FBS, and respective antibiotics were purchased from Merck, India. The fluorescence dye AO and EB were procured from Invitrogen. The MCF-7 breast cancer cells were supplied by NCCS, Pune, India.

PREPARATION OF PLANT EXTRACT [18]

5g of powdered *Cleome gynandra* leaves were mixed in 100 mL of distilled water and boiled at a constant temperature of 60^{o}C for 25 minutes and further followed by cooling under ambient temperature. This *Cleome gynandra* leaves extract solution was filtered using Whattman no. 1 filter paper. This filtrate contains bioactive agents or compounds that act as a reducing agent, where bulk silver ions change to nanostructured silver particles during the green synthesis process.

Journal of Chemical Health Risks
www.jchr.org
JCHR (2024) 14(5), 235-247 | ISSN:2251-6727

SILVER NITRATE ($AgNO_3$) 1mM PREPARATION

1mM of $AgNO_3$ was added to 100 mL of distilled water, followed by a forceful stirring method to prepare $AgNO_3$ solution, which contained micro-structured silver ions that were converted into nanostructured silver particles by green synthesis.

BIOSYNTHESIS OF AgNPs

Using plants as precursor molecules, the silver nanoparticle was successfully produced in this study. According to recent research [18]. For methodology, 0.1 mL of plant extract plus 0.9 mL of 1 mM silver nitrate were taken together in a fresh sterile test tube and held in a room atmosphere for 1 h. The colour formation was monitored, which turned from pale yellow to reddish-brown colour through the naked eye observation, indicating the presence of silver nanoparticles. Next, the colour-changed solution was dried in air and washed with distilled water using a hot air oven at 45^0C for 1 day. The collected powder samples were maintained in a deep freezer for further experiments.

LYOPHILIZATION PROCESS

The synthesized nanoparticles were lyophilized (freeze-drying) to improve stability, especially during long-term storage and offer new routes of administration in solid-state.

CHARACTERIZATION OF SILVER NANOPARTICLES

Scanning Electron Microscope Analysis of AgNPs.

The green synthesized AgNPs were characterized by SEM (Hitachi S-4500 SEM apparatus). By simply dropping a tiny amount of the sample onto a copper grid that has been coated with carbon, thin films of the sample were created. The extra solution was then blotted away, and the film on the SEM grid was then left to dry for 5 minutes under a mercury lamp [19].

FTIR spectroscopy analysis

The FTIR spectra of all the synthesized NPs were obtained using an FTIR spectrometer with a frequency range of 400 to 4000 cm−1 with an (IR-grade Potassium Bromide) KBr pellet. The pellet was obtained by mixing 200:1 of KBr and NPs. The KBr mixture was crushed using mortar and pestle, and the pellet was gained using a hydraulic pellet maker.

UV-Visible spectrophotometer analysis

UV-visible spectrum analysis for AgNPs was carried out. The change in colour of the reaction mixture was recorded by visual observation. The reduction of silver nitrate to silver nanoparticles was analysed by measuring the UV-vis spectra of the solution. The absorption spectrum of the sample was taken in the range of 300-500 nm using Thermo scientific UV–vis spectrophotometer.

DLS measurements

The Malvern Zetasizer was used to measure the average hydrodynamic diameter and particle size distribution of AgNPs (Malvern Instruments Ltd, Malvern, UK). Zetasizer software was used to analyze the acquired data.

Photoluminescence analysis

The Photoluminescence analysis was performed by measuring the intensity by Cary Eclipse, Agilent Technologies, and Singapore.

ASSAYS FOR ANTIOXIDANT ACTIVITY

DPPH (2, 2-DIPHENYL-PICRYL HYDRAZYL)

DPPH was performed by the method [20]. The assay was performed using green synthesized AgNPs, dissolved in methanol. 0.5mM DPPH solution in methanol was prepared and 0.5ml of this DPPH solution was mixed with 0.1ml of various concentration ((50, 100, 150, 200, and 250µg/ml) of the green synthesized AgNP and mixed thoroughly, then 4ml of methanol was added and allowed to stand in a darkroom for 30 min. The absorbance was measured at 517nm in UV spectrophotometer (Perkin Elmer). Decrease in absorbance of the DPPH solution indicates an increase in radical scavenging activity. The ability of the silver nanoparticles to scavenge DPPH was calculated using the following formula.

$$Percentage\ scavenged = \frac{Absorbance\ of\ control - Absorbance\ of\ test}{Absorbance\ of\ control} \times 100$$

Hydrogen peroxide radical scavenging assay

A solution of freshly prepared 4 mM hydrogen peroxide in 0.1 M phosphate buffer (pH 7.4) was used in this assay. 850µL of green synthesized AgNPs solution of varying concentrations (50, 100, 150, 200, and 250µg/mL) was added to 150µL of prepared H_2O_2 solution in phosphate buffer. The tubes were then kept aside for 10 minutes and the absorbance is read at 230nm. Ascorbic acid was used as positive control and the experiment was carried out in triplicates [21].

Journal of Chemical Health Risks
www.jchr.org
JCHR (2024) 14(5), 235-247 | ISSN:2251-6727

Ferric ion Reducing power assay

In a series of test tubes, varying volumes of sample solution (50 to 250µg/mL) were added and adjusted to 1mL with ethanol. To each tube, 2.5 mL PO_4 buffer and potassium ferric cyanide were added. A blank was prepared by 3 mL of PO_4 buffer alone. The tubes were then incubated at 50° C for 20 minutes in boiling bath. After incubation, 2.5 mL of 10% TCA was introduced into each tube, followed by centrifugation at 3000rpm for 15 minutes. Then, 0.5mL of distilled H_2O and ferric chloride were introduced to all the tubes, and the resulting colour was read at 700nm [22, 23].

ASSAYS FOR ANTICANCER ACTIVITIES

Maintenance of Cell

The human breast adenocarcinoma cell lines (MCF-7) were obtained from the National Centre for Cell Science (NCCS), Pune, India, and grown in Eagles Minimum Essential Medium containing 10% fetal bovine serum (FBS). The cells were maintained at 37ºC, 5% CO_2, 95% air and 100% relative humidity.

MTT assay

Viable MCF-7 cells were plated in a 96-well micro plate at a cell density of $1x10^6$ cells/mL and allowed to grow in a CO_2 incubator at 37 °C for 24 hours (5% CO_2). The medium was replaced after the period of incubation and the MCF-7 cells were treated with the AgNPs at different concentrations of 50, 100, 150, 200 and 250µg/mL. Following a 24-hour incubation period, the samples were examined and photographs of the morphological differences between treated and untreated cells were taken using an inverted microscope (Magnus INVI; 20 magnification). After being washed with phosphate-buffered saline (PBS, pH 7.4), the cells were loaded to each well with 20µL of MTT solution (5 mg/mL), and they were then left in the dark at 37°C for an additional 4 hours. Following the addition of 100µL of DMSO to dissolve the formazan crystals, an ELISA plate reader was used to read the absorbance spectroscopically in the 570 nm range **[24]**.

$$Cell\ viability\ (\%) = \frac{Absorbance\ of\ treated\ cells}{Absorbance\ of\ control\ cells} \times 100$$

DNA Fragmentation Assay [25]

In a 6-well plate, $4x10^6$ cells were incubated with varying drug concentrations of AgNPs (10^5 target cells per well) for 24 hrs at 37ºC with 5 % CO_2. After incubation, the cells were pelleted and lysed in 0.5 mL detergent buffer, 5 mM EDTA, and 0.2% Triton. Incubated on the ice for about 30 minutes after properly vortexed. Centrifuged for 30 minutes at 27,000 x g, then split the supernatants into two 250 µl of aliquot parts. Finally, 50 µl of ice-cold 5 M NaCl was added to each aliquot and vortexed thoroughly. Pipetted 600µL of ethanol and 150µL of 3 M sodium acetate, pH 5.2, to the mixture. The tubes were maintained at -80°C for one hour and centrifuged at 20,000 x g for 20 minutes; carefully discarded the supernatants. Resolved the pellets in 400µL of extraction buffer to combine the DNA extracts (10 mM Tris and 5 mM EDTA). Included 2 µL of 10 mg/mL DNase-free RNase and left standing at 37°C for 5 hours. Added 40 µL of buffer (100 mM Tris pH 8.0, 100 mM EDTA, and 250 mM NaCl) and 25 µL of proteinase K at 20 mg/mL. Incubated at 65°C overnight. Extracted DNA using phenol, chloroform, and isoamyl alcohol (25:24:1), ethanol was then used to precipitate. Carefully discard the supernatant without disturbing the pellet.

After the pellet had been air-dried, it was resuspended in 20µL of Tris-acetate EDTA buffer. An aliquot was added with 2µL of loading buffer and loaded onto the wells. The DNA samples were electrophoresed on a 2 % agarose gel with 1µg/mL ethidium bromide and analyzed using a UV transilluminator.

RESULT AND DISCUSSION

CHARACTERIZATION OF SILVER NANOPARTICLES

Silver nitrate solution is colourless, and after adding *Cleome gynandra* plant extract, the colourless silver nitrate solution became reddish brown in colour. This confirmed that the silver nitrate was reduced and transformed into silver nanoparticles.

Scanning Electron Microscope analysis

High-magnification images of AgNPs were obtained using the SEM technique. This technique can determine morphological features (number, dimension, and shape) of small particles by scanning reflections of a focused beam of electrons over the particles' surfaces. SEM images (Figure 1a,b) of the particles showed rod-shaped particles having different average diameters D1 (125.62nm), D2 (156.32nm), D3 (172.74nm), D4 (141.38nm), D5 (134.34nm), D6 (113.19), D7 (90.04nm), D8 (135.94nm), D9 (110.72nm), D10

Journal of Chemical Health Risks
www.jchr.org
JCHR (2024) 14(5), 235-247 | ISSN:2251-6727

(145.98nm) and D11 (125.62nm) with smooth surface morphology, and well scattered with a nearly compact arrangement. According to previous literature [26], the silver nanoparticle synthesized from *Euphorbia prostrates* was also rod-shaped.

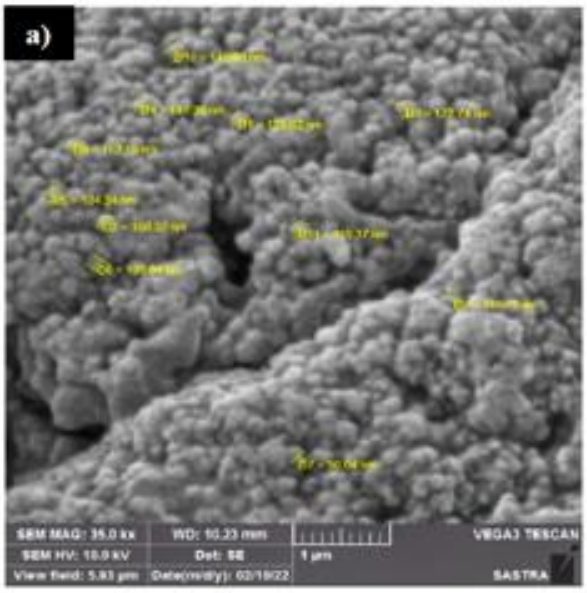

Figure 1a. SEM analysis of AgNPs (172.74nm to 90.04nm size of AgNPs)

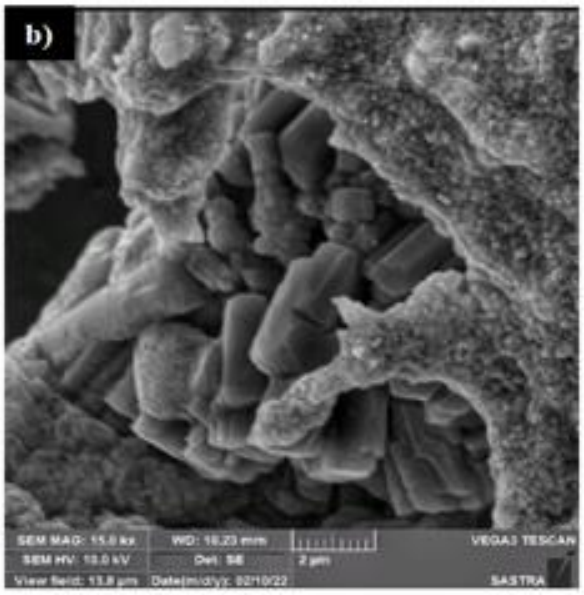

Figure 1b. SEM analysis of AgNPs (Rod Shaped AgNPs)

FTIR Spectroscopy analysis

Figure 2 depicts the FTIR spectrum of the produced AgNPs. This spectrum indicates possible biomolecules in the leaf extract responsible for silver ion reduction and interaction with AgNPs. AgNPs have strong IR bands at 3403.26, 2921.61, 1598.58, 1384.37, 1021.21, and 606.91 cm-1. The extensive band at 3403.26 cm-1 corresponds to stretching vibration of (O-H) of phenolic [27], 2921.61 cm-1 indicating the existence of the functional group (C-H) [28], 1598.58 cm-1 indicates the existence of the functional group (C=O) [29], 1384.37 cm-1 indicates the existence of the functional group (N=O) [30], 1021.21 cm-1 indicates functional group (C-C) [31], and 606.19 cm-1 indicates functional group (C-Cl) [32]. Thus, based on the IR spectra, it may be assumed that these biomolecules play a role in bioreduction as well as biosynthetic stability of the silver nanoparticles.

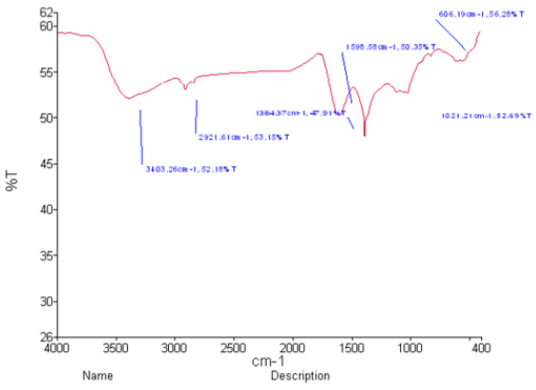

Figure 2. FTIR spectroscopy analysis of AgNPs

UV-Visible absorption spectrum of AgNPs.

The existence of NS-AgNPs was confirmed in the sample using UV-VIS spectra analysis. Usually, NS-AgNPs in aqueous solution absorb radiation around 430nm, appearing reddish brown, as reported in previous studies [33]. The UV -Vis spectrum was used to confirm the existence of NS-AgNPs by showing surface plasmon resonance (SPR) peaks around 400nm (figure 3).

Journal of Chemical Health Risks
www.jchr.org
JCHR (2024) 14(5), 235-247 | ISSN:2251-6727

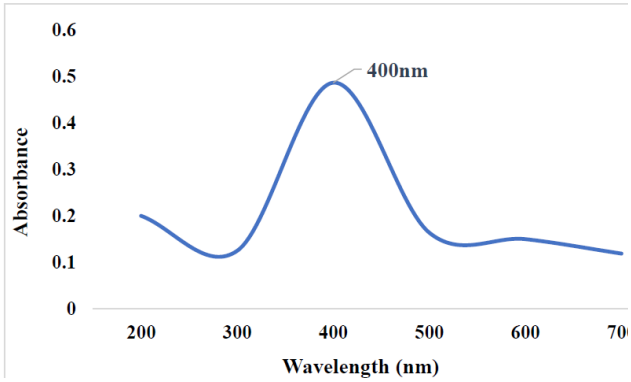

Figure 3. UV-VIS absorption spectrum of AgNPs

DLS Measurements

The AgNPs measured 526 nm in size (figure 4). The size of the produced nanoparticles was greater than the expected range of 1-100nm. Due to the protein that was linked to the surface of the nanoparticles, size was greater than what was desired. The study reported by Roy and Bharadvaja, 2017 [34] specified that the silver nanoparticles made from *Plumbago zeylanica* were 500 nm in size.

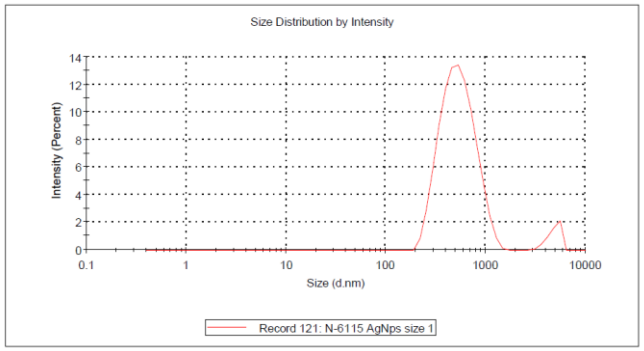

Figure 4. Zeta size distribution

(The peak revealed the size of AgNPs is 526nm)

The generated silver nanoparticles had a negative zeta potential. The zeta potential i=was discovered to be -18.2mV (figure 5). The zeta potential plays an important role in influencing the stability of aqueous nanosuspensions. Zeta potential values of at least ±30 mV are required for the indicator of stable nanosuspension [35]. As a result, this discovery revealed that the particles' electrostatic properties has kept them reasonably stable.

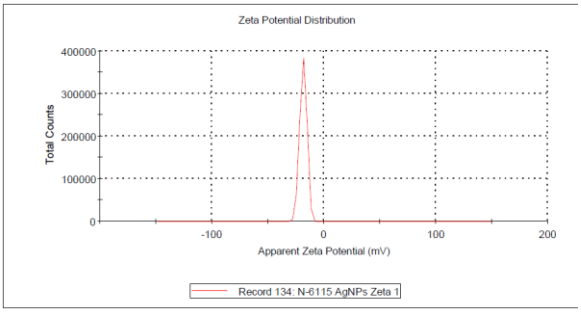

Figure 5. Zeta potential distribution (i= of AgNPs is -18.2mV)

Photoluminescence analysis

Photoluminescence spectra of synthesized silver nanoparticles were carried out to evaluate their optical property. Figure 6 displayed the excitation peak at 397.07nm, while the emission peak was observed at 579.85nm. The excitation peak at 397.07nm very well correlates with absorption maxima recorded with the UV-VIS spectrophotometer (400nm). Similar studies in the past [36] have detected an excitation peak at 414 nm whereas an emission peak was observed at 576nm.

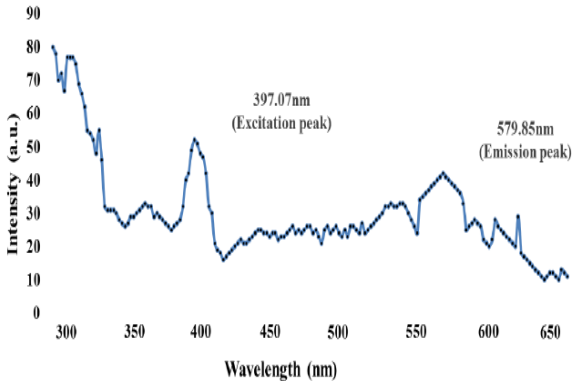

Figure 6. Photoluminescence analysis of AgNPs. (Excitation and emission peak at 397.07nm and 579.85nm)

ANTIOXIDANT EFFICIENCY OF SILVER NANOPARTICLES

DPPH Radical Scavenging Assay

In-vitro antioxidant activity was measured using a DPPH test. It is a stable organic radical type frequently used to gauge how well natural antioxidants scavenge free radicals [37]. The IC_{50} value is used to represent the outcomes (amount of antioxidants necessary to decrease initial DPPH concentration by 50%). In the present study, the percentage of inhibition was found to increase with

Journal of Chemical Health Risks
www.jchr.org
JCHR (2024) 14(5), 235-247 | ISSN:2251-6727

the increase in AgNP concentration. At 250 µg/ml, the maximum inhibition of 82.5 percent was observed, and ascorbic exhibited 88.33 % inhibition (Figure 7). The IC_{50} value for the AgNPs was determined to be 165.26 µg/ml. As a result, it could be safely concluded that the silver nanoparticles produced from the extract of *Cleome gynandra* leaves have very good free radical scavenging action.

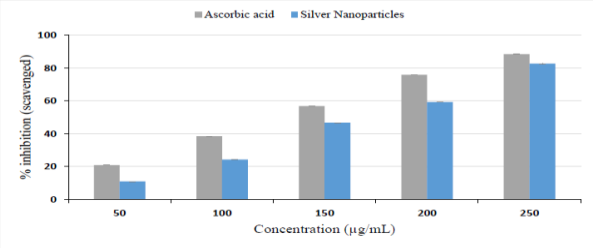

Figure 7. DPPH free radical scavenging activity of the AgNPs.
IC_{50} of AgNPs is = 165.26µg/mL.

Hydrogen peroxide radical scavenging activity

In-vitro antioxidant activity of AgNPs was determined by hydrogen peroxide (H_2O_2) radical scavenging assay. Maximum scavenging activity at 75.21% and 84.18% at 250 ug/ml was observed for AgNPs and standard ascorbic, respectively (Figure 8). Therefore, the results of this study also indicate that the silver nanoparticles synthesized from the extract of *Cleome gynandra* leaves had excellent free radical scavenging capacity. Previous studies [38] have determined the hydrogen peroxide scavenging activity of *Catharanthus roseus* extract, CrAgNPs, and Vitamin C. The results showed that *C. roseus* extract, CrAgNPs, and Vitamin C had 55.45%, 72.34%, and 66.25% of antioxidant activity, respectively.

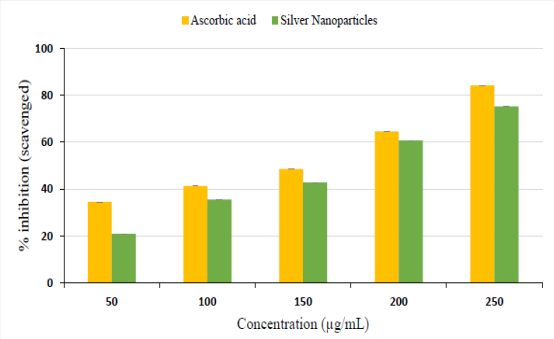

Figure 8: Hydrogen peroxide assay of the AgNPs.
IC_{50} of AgNPs was observed at 161.47 µg/mL

Ferric ion Reducing power assay

The AgNPs antioxidant activity was measured by the reducing power assay. The percentage of inhibition increased with the concentration of silver nanoparticles. At 250 µg, there was a 75.86% inhibition, ascorbic acid exhibited 75.38 % inhibition (Figure 9), and the IC50 value of AgNPs was found to be 145.70 µg/mL. Based on the results obtained, it could be concluded that the silver nanoparticles synthesized from the extract of *Cleome gynandra* leaves have the potential to neutralize free radicals. Researchers in the past [39] have observed that strong antioxidant activity was determined by reducing power assay on synthesized silver nanoparticles using *Lippia nodiflora* aerial extract, and the reducing activity of AgNPs was found to increase with increasing concentrations. Another article [40] suggested that the scavenging capacity test was the best choice for the measurement of antioxidant activity because of its ability (in a radical form), simplicity, and fast assay. Our results are in line with the previous findings [41].

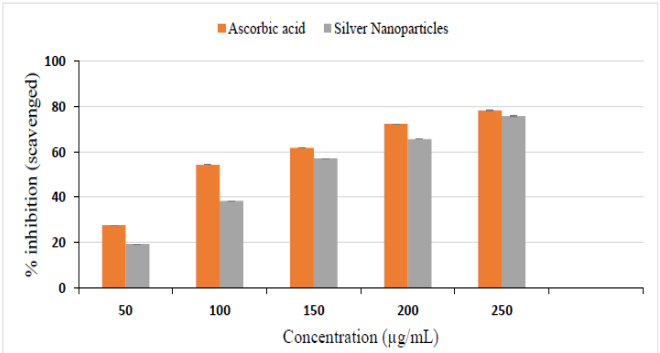

Figure 9: Reducing power assay of the AgNPs.
IC_{50} of AgNPs was observed at 145.70 µg/mL

***IN VITRO* ANTICANCER ACTIVITIES**
MTT assay

The cytotoxic potency of produced AgNPs on MCF-7 cells was determined by MTT assay. After incubation of cells, the maximal cytotoxic effect was detected as cell death by apoptosis with nuclear segmentation. This assay was used to identify the percentage of viability after treatment with AgNPs at various concentrations (15.625, 31.25, 62.5, 125, 250ug/mL) on the MCF 7 cell line. Figures 10 & 11 show that the treatment with nanoparticles drastically reduced the percent of cell viability in a concentration-dependent

Journal of Chemical Health Risks
www.jchr.org
JCHR (2024) 14(5), 235-247 | ISSN:2251-6727

manner. On MCF-7 cells, the IC_{50} value of AgNPs was 158.25ug/ml. The findings of this study are in accordance with previous studies that proved the anti-cancer activity of AgNPs derived from *Cleome gynandra* leaf extract on the breast cancer cell line. The mechanism of silver nanoparticles' anticancer effect consists of either AgNPs entering the cell, which causes damage by forming a stable S-Ag bond with an enzyme's thiol group and deactivating it, or the breaking of hydrogen bonds between nitrogen bases in DNA, which denaturizes it [42, 43, 44]. In general, it was discovered that green AgNPs exhibit low or no toxicity to normal cells and broad activity against cancer cells in a concentration-dependent manner.

Researchers in the past [45] have studied that the biosynthesis AgNPs using the *Lonicera hypoglauca* flower extract caused the cytotoxicity of human breast cancer cells. Furthermore, AgNPs derived from the plants *Chaenomeles sinensis* and *Cibotium barometz* demonstrated anti-cancer action against breast cancer (MCF-7) [46]. According to a related study, exposure of cells to AgNPs may result in a variety of morphological alterations and a decrease in cell viability. In general, cellular morphological alterations in the cell may be caused by the cell's composition being disturbed by the interaction of AgNPs with the cell surface. When silver nanoparticles enter a cell, they cause damage by forming a stable S-Ag bond with an enzyme's thiol group, which renders the enzyme inactive. They can also denaturize DNA by rupturing the hydrogen bonds between its nitrogen bases [44].

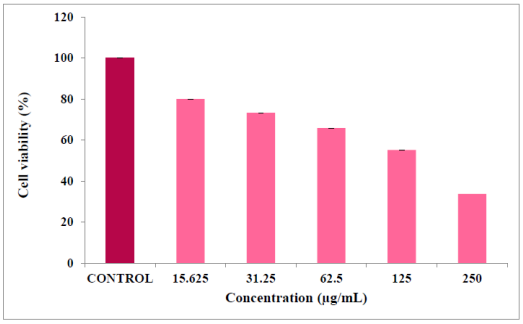

Figure 10: MTT assay of silver nanoparticle from *Cleome gynandra* against MCF-7 cell line. IC50 of the AgNPs - 158.25µg/mL

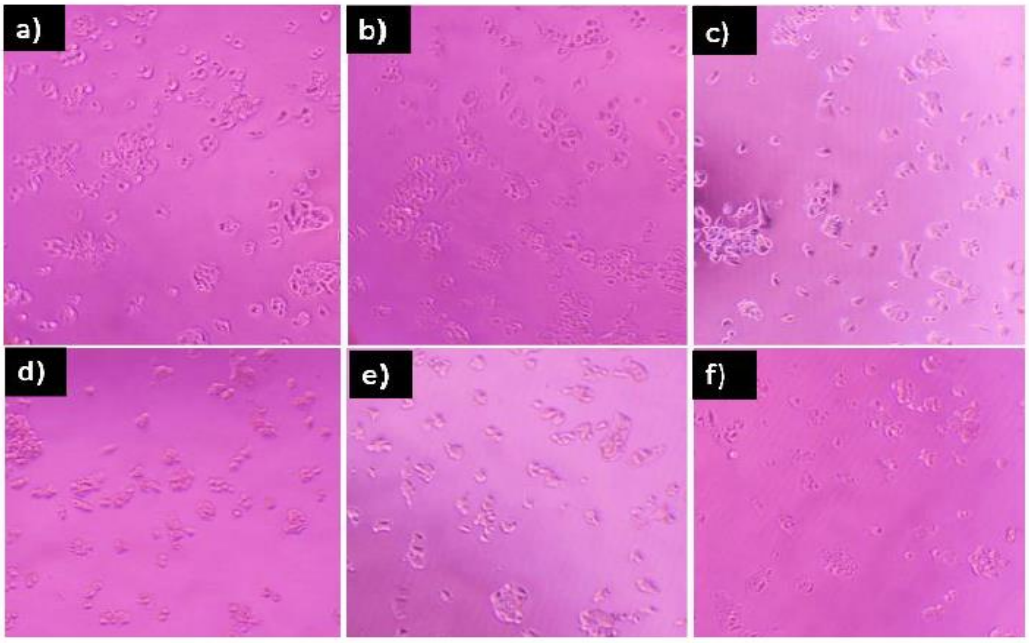

Figure 11. Cytotoxic activity of different concentrations of AgNPs against MCF-7 cells a) Control, b) AgNPs treated (15.62µg/mL), c) AgNPs treated (31.25 µg/mL), d) AgNPs treated (62.5 µg/mL), e) AgNPs treated (125 µg/mL) and f) AgNPs treated (250 µg/mL)

Journal of Chemical Health Risks
www.jchr.org
JCHR (2024) 14(5), 235-247 | ISSN:2251-6727

DNA fragmentation analysis

DNA fragmentation is generally regarded as an indicator of apoptosis. Although the precise mechanism for this contact is not yet established, nanoparticles can easily pass the nuclear membrane and interact with DNA either directly or indirectly [25]. The DNA fragmentation test was used to examine how AgNPs made from *Cleome gynandra* leaf extract affected the induction of apoptosis in human breast cancer cells. The human breast cancer cells were exposed for 24 hours to effective concentrations of samples 500µg ml-1 and 1000µg ml-1 to investigate the effect of AgNPs on DNA damage. On an agarose gel, DNA was then electrophoresed after being extracted from treated and control cells (1.5 percent). The findings demonstrated that AgNPs caused apoptosis in human breast cancer cells by cleaving the nuclear DNA in a ladder pattern (Figure 12). Untreated control cells did not display any DNA fragmentation. AgNPs-treated cells experienced apoptosis along with a drop in the proportion of G0/G1 cells and a rise in the proportion of G2/M cells, indicating G2/M cell cycle arrest [47]. ROS are signal molecules that accelerate cell cycle progression and have the potential to damage DNA oxidatively [48]. Two signs that indicate apoptosis include DNA fragmentation and an uneven decline in cell size, resulting in shrunken and reduced cells. In the current study, DNA extraction from MCF-7 cells treated with varied quantities of AgNPs and detection of it in an agarose gel were used to confirm DNA fragmentation. Fig.12 unequivocally demonstrates that the DNA "laddering" pattern is one of the factors contributing to cell death in MCF-7 cells treated with AgNPs. According to a similar study [49, 50], reactive oxidative species and nanoparticles both damage DNA and activate the p53 and other DNA repair proteins, imitating the effects of radiation on the development of cancer.

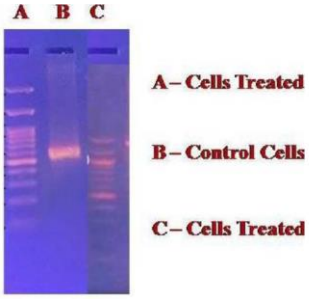

Figure 12: DNA "Laddering" pattern in AgNPs treated MCF-7 cells

A-Cells treated with 500 µg/mL^{-1}; B – Control; µg/mL^{-1}
C-Cells treated with 1000 µg/mL^{-1}

Conclusion

The biosynthesized silver nanoparticles in the field of nano-biotechnology have increased the significance of developing environmentally acceptable, economically viable, stable nanoparticles, and their applications in electronics, agriculture, and medicine are expanding. In the present study, the green synthesis method was employed to synthesize silver nanoparticles, and this was confirmed by color change, characterization, and absorption spectra examined with UV-VIS spectrophotometry, zeta particle size distribution, zeta potential distribution, FTIR, SEM, and photoluminescence. The compounds that caused silver nitrate to be reduced to silver ions were examined using FTIR spectroscopy. The synthesized silver nanoparticles were assessed for their free radical scavenging activity and found to have significant antioxidant activity. Interestingly, the AgNPs were found to decrease MCF - 7 cell viability in a concentration-dependent manner for 24 hrs, and it is further supported by DNA fragmentation in the MCF-7 cell line. The results of this study confirm the antioxidant and anticancer activities of synthesized AgNPs.

References

1. Shabaani, M.; Rahaiee, S.; Zare, M.; Jafari, S. M. Green Synthesis of ZnO Nanoparticles Using Loquat Seed Extract; Biological Functions and Photocatalytic Degradation Properties. *LWT* **2020**, *134*, 110133.
2. Sarkar, S.; Kotteeswaran, V. Green Synthesis of Silver Nanoparticles from Aqueous Leaf Extract of Pomegranate (Punica granatum) and Their Anticancer Activity on Human Cervical Cancer Cells. *Adv. Nat. Sci.: Nanosci. Nanotechnol.* **2018**, *9* (2), 025014.
3. Xu, L.; Wang, Y. Y.; Huang, J.; Chen, C. Y.; Wang, Z. X.; Xie, H. Silver Nanoparticles: Synthesis, Medical Applications and Biosafety. *Theranostics* **2020**, *10* (20), 8996–9031.
4. Gavas, S.; Quazi, S.; Karpiński, T. M. Nanoparticles for Cancer Therapy: Current

Progress and Challenges. *Nanoscale Res. Lett.* **2021**, *16*, 173.

5. Kareem, M.; Babu, H.; Lakshmi, G. V. Anticancer, Antibacterial, Antioxidant, and Photo-Catalytic Activities of Eco-Friendly Synthesized Ni Nanoparticles. *Inorg. Chem. Commun.* **2023**, *148*, 110274.
6. Gavas, G. N.; Chackaravarthi, G.; Ramachandran, G.; Chelliah, C. K.; Maruthupandy, M.; Alharbi, M. S.; Alharbi, N. S.; Khaled, J. M.; Li, W. J. Morphological Damage and Increased ROS Production of Biosynthesized Silver Nanoparticles Against MCF-7 Breast Cancer Cells Through In Vitro Approaches. *J. King Saud Univ. Sci.* **2022**, *34*, 101795.
7. Rajabnia, T.; Meshkini, A. Fabrication of Adenosine 5'-Triphosphate-Capped Silver Nanoparticles: Enhanced Cytotoxicity Efficacy and Targeting Effect Against Tumor Cells. *Process Biochem.* **2018**, *65*, 186–196.
8. Ebrahimzadeh, M. A.; Naghizadeh, A.; Amiri, O.; Shirzadi-Ahodashti, M.; Mortazavi-Derazkola, S. Green and Facile Synthesis of Ag Nanoparticles Using Crataegus Pentagyna Fruit Extract (CP-AgNPs) for Organic Pollution Dyes Degradation and Antibacterial Application. *Bioorg. Chem.* **2020**, *94*, 103425.
9. Kim, C. G.; Castro-Aceituno, V.; Abbai, R.; Lee, H. A.; Simu, S. Y.; Han, Y.; Hurh, J.; Kim, Y. J.; Yang, D. C. Caspase-3/MAPK Pathways as Main Regulators of the Apoptotic Effect of the Phyto-Mediated Synthesized Silver Nanoparticle from Dried Stem of *Eleutherococcus senticosus* in Human Cancer Cells. *Biomed. Pharmacother.* **2018**, *99*, 128–133.
10. Lakhan, M. N.; Chen, R.; Shar, A. H.; Chand, K.; Shah, A. H.; Ahmed, M.; Ali, I.; Ahmed, R.; Liu, J.; Takahashi, K.; Wang, J. Eco-Friendly Green Synthesis of Clove Buds Extract Functionalized Silver Nanoparticles and Evaluation of Antibacterial and Antidiatom Activity. *J. Microbiol. Methods* **2020**, *173*, 105934.
11. Huang, H.; Lai, W.; Menghua, C.; Liang, L. An Evaluation of Blood Compatibility of Silver Nanoparticles. *Sci. Rep.* **2016**, *6* (1), 25518.
12. Tripathi, D.; Tripathi, A.; Singh, S. S.; Singh, Y.; Vishwakarma, K.; Yadav, G.; Sharma, S.; Singh, V. K.; Mishra, R. K.; Upadhya, R. G.; Dubey, N. K.; Lee, Y.; Chauhan, D. K. Uptake, Accumulation and Toxicity of Silver Nanoparticle in Autotrophic Plants, and Heterotrophic Microbes: A Concentric Review. *Front. Microbiol.* **2017**, *8*, 07.
13. Singh, A.; Gautam, P. K.; Verma, A.; Singh, V.; Shivapriya, P.; Shivalkar, S.; Kumar, A.; Sintu, S.; Samanta, K. Green Synthesis of Metallic Nanoparticles as Effective Alternatives to Treat Antibiotics Resistant Bacterial Infections: A Review. *Biotechnol. Rep.* **2020**.
14. Govindan, L.; Sathiyaseelan, A.; Kalaichelvan, P. T.; Murugesan, K. Plant-Mediated Synthesis of Silver Nanoparticles Using Fruit Extract of *Cleome viscosa* L.: Assessment of Their Antibacterial and Anticancer Activity. *KIJOMS* **2017**, *4* (1).
15. Danjie, Z.; Govindan, R.; Ramzi, A. M.; Nasir, A. S.; Riaz, U.; Omer, M. A.; Govindan, R.; Natesan, M. Marine Algae *Caulerpa Taxifolia* Mediated Silver Nanoparticles Enhances the Anti-Cancer Activity Against A549 Lung Cancer Cell Line Through Cytotoxicity Effect/Morphological Damage. *Saudi J. Biol. Sci.* **2020**, *27*, 3421–3427.
16. Shah, Z.; Hassan, S.; Shaheen, K.; Khan, S. A.; Gul, T.; Anwar, Y.; Al-shaeri, M. A.; Khan, M.; Haleem, M. A.; Suo, H. Synthesis of AgNPs Coated with Secondary Metabolites of *Acacia nilotica*: An Efficient Antimicrobial and Detoxification Agent for Environmental Toxic Organic Pollutants. *Mater. Sci. Eng. C* **2020**, *111*, 110829.
17. Mohanta, Y. K.; Biswas, K.; Jena, S. K.; Hashem, A.; Abd-Allah, E. F.; Mohanta, T. K. Anti-Biofilm and Antibacterial Activities of Silver Nanoparticles Synthesized by the Reducing Activity of Phytoconstituents Present in the Indian Medicinal Plants. *Front. Microbiol.* **2020**, *11*, 1143.

Journal of Chemical Health Risks

www.jchr.org

JCHR (2024) 14(5), 235-247 | ISSN:2251-6727

18. Mani, M.; Harikrishnan, R.; Purushothaman, P.; Pavithra, S.; Rajkumar, P.; Kumaresan, S.; Dunia, A.; Farrajd, A. L.; Soliman, M.; Elshikhd, B.; Krishnan, B.; Balasubramanian, K.; Kaviyarasu, K. Systematic Green Synthesis of Silver Oxide Nanoparticles for Antimicrobial Activity. *Environ. Res.* **2021**, *202*, 111627.
19. Akhtar, K.; Ali Khan, S.; Bahadar Khan, S.; Asiri, A. M. Scanning Electron Microscopy: Principle and Applications in Nanomaterials Characterization. In *Handbook of Materials Characterization*; 2018; pp 113–145.
20. Saravanan, R.; Pemaiah, B.; Narayanan, M.; Ramalingam, S. Gas Chromatography–Mass Spectrometry Analysis, In Vitro Cytotoxic and Anti-Oxidant Efficacy on *Cleome gynandra* L. (Leaves): A Traditional Drug Sources. *Asian J. Pharm. Clin. Res.* **2017**, *3*, 84.
21. Nabavi, S. M.; Ebrahimpour, F.; Nabavi, S. F.; Hamidinia, A.; Bekhradnia, A. R. Determination of Antioxidant Activity, Phenol, and Flavonoids Content of *Parrotia persica* Mey. *Pharmacology Online* **2008**, *2*, 560–567.
22. Singh, S.; Singh, R. P. In Vitro Methods of Assay of Antioxidants: An Overview. *Food Rev. Int.* **2008**, *24*, 392–415.
23. Félix-Silva, J.; Souza, T.; Gomes Camara, R. B. B.; Cabral, B.; Silva-Júnior, A. A.; Rebecchi, I. M. M.; Zucolotto, S. M.; Oliveira Rocha, H. A.; Fernandes-Pedrosa, M. F. In Vitro Anticoagulant and Antioxidant Activities of *Jatropha gossypiifolia* L. (Euphorbiaceae) Leaves Aiming Therapeutical Applications. *BMC Complement Altern. Med.* **2014**, *14*, 405.
24. Mossman, B. T. In Vitro Approaches for Determining Mechanisms of Toxicity and Carcinogenicity by Asbestos in the Gastrointestinal and Respiratory Tracts. *Environ. Health Perspect.* **1983**, *53*, 155-161.
25. Mariyappan, S.; Ramalingam, S.; Murugan, L.; Saravanan, R. Anti-Proliferative Potential of *Carica papaya* Leaves on Breast Cancer Cells – MCF-7. *J. Exp. Biol. Agric. Sci.* **2021**, *9*(5), 678–686.
26. Abduz Zahir, A.; Rahuman, A. Evaluation of Different Extracts and Synthesised Silver Nanoparticles from Leaves of *Euphorbia prostrata* Against *Haemaphysalis bispinosa* and *Hippobosca maculata*. *Vet. Parasitol.* **2021**, *187*(3-4), 511-520.
27. Devanesana, S.; Jayamala, M.; AlSalhi, M. S.; Umamaheshwari, S.; Jacob, A. A.; Ranjitsingh, A. Anti-Microbial and Anticancer Properties of *Carica papaya* Leaves Derived Di-Methyl Flubendazole Mediated Silver Nanoparticles. *J. Infect. Public Health* **2021**, *14*, 577–587.
28. Jyoti, K.; Baunthiyal, M.; Singh, A. Characterization of Silver Nanoparticles Synthesized Using *Urtica dioica* Linn. Leaves and Their Synergistic Effects with Antibiotics. *J. Radiat. Res. Appl. Sci.* **2016**, *9*, 217-227.
29. Saravanakumar, K.; Peng, M. M.; Ganesh, M.; Jayaprakash, J.; Mohankumar, M.; Jang, H. T. Low-Cost and Eco-Friendly Green Synthesis of Silver Nanoparticles Using *Prunus japonica* (Rosaceae) Leaf Extract and Their Antibacterial, Antioxidant Properties. *Artif. Cells Nanomed. Biotechnol.* **2017**, *45*(6), 1165-1171.
30. Sreekanth, T. V. M.; Jung, M. J.; Eom, I. Y. Green Synthesis of Silver Nanoparticles Decorated on Graphene Oxide Nanosheets and Their Catalytic Activity. *Appl. Surf. Sci.* **2015**, *361*, 1-6.
31. Krishnan, V.; Bupesh, G.; Manikandan, E.; Arul, K.; Thanigai, S.; Magesh, S.; Kalyanaraman, R. Green Synthesis of Silver Nanoparticles Using *Piper nigrum* Concoction and Its Anticancer Activity Against MCF-7 and Hep-2 Cell Lines. *J. Antimicrob. Agents* **2016**, *2*, 123-128.
32. Bagherzade, G.; Tavakoli, M. M.; Namaei, M. H. Green Synthesis of Silver Nanoparticles Using Aqueous Extract of Saffron (*Crocus sativus* L.) Wastages and Its Anti-Bacterial Activity Against Six Bacteria. *Asian Pac. J. Trop. Biomed.* **2017**, *7*(3), 231-237.
33. Saravanakumar, K.; Wang, M. H. Trichoderma-Based Synthesis of Anti-Pathogenic Silver Nanoparticles and Their Characterization, Antioxidant, and Cytotoxicity Properties. *Microb. Pathog.* **2018**, *114*, 269-273.
34. Roy, A.; Bharadvaja, N. Silver Nanoparticles Synthesis from a Pharmaceutically Important

Journal of Chemical Health Risks

www.jchr.org

JCHR (2024) 14(5), 235-247 | ISSN:2251-6727

Medicinal Plant *Plumbago zeylanica*. *MOJ Bioequiv. Bioavailab.* **2017**, *3*(5), 118-121.

35. Rajendran, R.; Mani, R. Photocatalytic, Antibacterial, and Anticancer Activity of Silver-Doped Zinc Oxide Nanoparticles. *J. Saudi Chem. Soc.* **2020**, *24*, 1010–1024.
36. Prasad, K. S.; Pathak, D.; Patel, A.; Dalwadi, P.; Prasad, R.; Patel, P.; Selvaraj, K. Biogenic Synthesis of Silver Nanoparticles Using *Nicotiana tobaccum* Leaf Extract and Study of Their Antibacterial Effect. *Afr. J. Biotechnol.* **2011**, *10*(41), 8122-8130.
37. Sagar, B.; Kedare, S. B.; Singh, R. P. Genesis and Development of DPPH Method of Antioxidant Assay. *J. Food Sci. Technol.* **2011**, *48*(4), 412–422.
38. Keshari, A. K.; Srivastava, A.; Chowdhury, S.; Srivastava, R. Antioxidant and Antibacterial Property of Biosynthesized Silver Nanoparticles. *Nanomed. Res. J.* **2021**, *6*(1), 17-27.
39. Sudha, A.; Jeyakanthan, J.; Srinivasan, P. Green Synthesis of Silver Nanoparticles Using *Lippia nodiflora* Aerial Extract and Evaluation of Their Antioxidant, Antibacterial, and Cytotoxic Effects. *Resource-Efficient Technol.* **2017**, *3*(4), 506-515.
40. Flaih, L. S.; Al-Saadi, N. H. Green Synthesis of Silver Nanoparticles from *Cassia obtusifolia* Leaves Extract: Characterization and Antioxidant Activity. *AIP Conf. Proc.* **2020**, *2290*, 060011.
41. Inbathamizh, L.; Mekalai Ponnu, T.; Mary, E. Jancy. In Vitro Evaluation of Antioxidant and Anticancer Potential of *Morinda pubescens* Synthesized Silver Nanoparticles. *J. Pharm. Res.* **2013**, *6*(1), 32–38.
42. Parveen, A.; Rao, S. Cytotoxicity and Genotoxicity of Biosynthesized Gold and Silver Nanoparticles on Human Cancer Cell Lines. *J. Clust. Sci.* **2015**, *26*, 775–788.
43. Soshnikova, V.; Kim, Y. J.; Singh, P.; Huo, Y.; Markus, J.; Ahn, S. Cardamom Fruits as a Green Resource for Facile Synthesis of Gold and Silver Nanoparticles and Their Biological Applications. *Artif. Cells Nanomed. Biotechnol.* **2018**, *46*(1), 108-117.
44. Shriniwas, P. P.; Subhash, T. K. Antioxidant, Antibacterial, and Cytotoxic Potential of Silver Nanoparticles Synthesized Using Terpenes-Rich Extract of *Lantana camara* L. Leaves. *Arch. Biochem. Biophys.* **2017**, *623*, 68-75.
45. Janga, S. J.; Yang, I. J.; Tettey, C. O.; Kim, K. M.; Shin, H. M. In Vitro Anticancer Activity of Green Synthesized Silver Nanoparticles on MCF-7 Human Breast Cancer Cells. *Mater. Sci. Eng.* **2016**, *68*, 430-435.
46. Sriranjani, R.; Srinithya, B.; Vellingiri, V.; Brindha, P.; Anthony, S. P.; Subramanian, A. S.; Muthuraman, M. Silver Nanoparticle Synthesis Using *Clerodendrum phlomidis* Leaf Extract and Preliminary Investigation of Its Antioxidant and Anticancer Activities. *J. Mol. Liq.* **2016**, *220*, 926-930.
47. Lee, Y. S.; Kim, D. W.; Lee, Y. H.; Oh, J. H.; Yoon, S.; Choi, M. S.; Lee, S. K.; Kim, J. W.; Lee, K.; Song, C. W. Silver Nanoparticles Induce Apoptosis and G2/M Arrest via PKCζ-Dependent Signaling in A549 Lung Cells. *Arch. Toxicol.* **2011**, *85*, 1529–1540.
48. Gonzalez, R. A.; Spring, H.; Müller, M.; Bürkle, A. Selective Loss of Poly(ADP-Ribose) and the 85-kDa Fragment of Poly(ADP-Ribose) Polymerase in Nucleoli During Alkylation-Induced Apoptosis of HeLa Cells. *Cell Metab.* **1999**, *274*(45), 32122-32126.
49. Kalishwaralal, K.; Sriram, M. I.; Kanth, S. B. M.; Gurunathan, S. Antitumor Activity of Silver Nanoparticles in Dalton's Lymphoma Ascites Tumor Model. *Int. J. Nanomedicine* **2010**, *5*, 753–762.
50. Mroz, R. M.; Schins, R. P.; Li, H.; Jimenez, L. A.; Drost, E. M.; Holownia, A.; MacNee, W.; Donaldson, K. Nanoparticle-Driven DNA Damage Mimics Irradiation-Related Carcinogenesis Pathways. *Eur. Respir. J.* **2008**, *31*, 241–251.